Nanoscale Horizons

Accepted Manuscript

ROYAL SOCIETY OF CHEMISTRY

rsc.li/nanoscale-horizons

Nanoscale Horizons

COMMUNICATION

Nuclear quantum tunnelling and carrier delocalization effects to bridge the gap between hopping and bandlike behaviors in organic semiconductors†

Received 00th January 20xx,
Accepted 00th January 20xx

DOI: 10.1039/x0xx00000x

www.rsc.org/

Yuqian Jiang,[a,b] Xinxin Zhong,[c] Wen Shi,[a] Qian Peng,[d] Hua Geng,[d] Yi Zhao[e]* and Zhigang Shuai[a,e]*

The experimental carrier mobility value of organic semiconductors increases rapidly in recent years to well exceed the theoretical limit based on hopping model calculated with the semi-classical Marcus theory, calling for better understanding and evaluation of carrier mobility. On the other hand, bandlike transport behavior has been observed for some ultra-pure and closely-packed organic single crystals. In this work, we identify the roles of quantum nuclear tunnelling and the charge delocalization effects, rendering a comprehensive computational approach to assess the carrier mobility for organic semiconductors. We present the first-principles evaluated mobility results for some representative organic transport materials at four levels ranging from semiclassical hopping to quantum nuclear enabled hopping and to quantum wavepacket diffusion, and eventually to the complete bandlike descriptions. We provide a comprehensive tool to assess the carrier mobility in organic semiconductors based on such improved understanding.

Remarkable progresses have been achieved in last decades in understanding and improving carrier mobility for organic semiconductors (OSCs) after intensive investigations on new materials, processes, and devices. Systems with hole mobility higher than 10 $cm^2V^{-1}s^{-1}$ have been discovered such as pentacene,[1] rubrene,[2] thienoacene derivatives[3] and electron mobility larger than 6 $cm^2V^{-1}s^{-1}$ such as naphthalene diimide derivatives [4] and perylene diimide derivatives [5] have also been produced. The bandlike behavior is usually applied to explain such high mobility OSCs, much as in inorganic semiconductors,[6] for example, band-like temperature-dependent mobility has been reported in pentacene,[7] rubrene,[8] N,N'-bis(n-$C_3F_7CH_2$)-(1,7 and 1,6)-dicyanoperylene-3,4:9,10- bis(dicarboximide)s (PDIF-CN2)[5] and 6,13-bis (triisopropylsilylethynyl)-pentacene (TIPS-P).[9] On the other hand, the well localized picture such as hopping process described by the semiclassical Marcus theory has gained tremendous popularity due to both the simplicity and the success in molecular design.[10] Such model is appropriate when the intermolecular transfer integrals are much smaller than the charge reorganization energy and the elementary charge transfer (CT) rate is described as:

$$k^{SC} = \frac{|V|^2}{\hbar}\left(\frac{\pi}{\lambda k_B T}\right)^{1/2} \exp\left(-\frac{\lambda}{4k_B T}\right) \quad (1)$$

A more elaborate hopping model was proposed by Nan *et al.* through incorporating the quantum nuclear effect[11] arising from multi-vibational modes, whereas the CT rate reads:

$$k^{QM} = \frac{|V|^2}{\hbar^2}\int_{-\infty}^{\infty} \mathrm{d}t \ \exp\left\{-\sum_j S_j\left[\left(2\bar{n}_j+1\right)-\bar{n}_j e^{-i\omega_j t}-\left(\bar{n}_j+1\right)e^{i\omega_j t}\right]\right\} \quad (2)$$

where $\bar{n}_j = 1/[\exp(\hbar\omega_j / k_B T)-1]$ is the occupation number for the *j*-th vibrational mode with frequency ω_j, and S_j is the Huang-Rhys factor relating to the *j*-th mode which represents the local electron-phonon coupling. In the limits of strong coupling $\sum_j S_j >> 1$, the short-time approximation $\exp(i\omega t) = 1 + i\omega t + (i\omega t)^2/2$, and high temperature $\hbar\omega_j / k_B T << 1$, $\bar{n}_j \approx k_B T / \hbar\omega_j$, Eq. (2) goes back to Eq. (1) with $\lambda = \sum_j \lambda_j = \sum_j S_j \hbar\omega_j$.

It is noted that even though Eq. (1) can correctly identify the essential molecular parameters, the calculated mobility values often underestimate the experiments. For example for pentacene, the Marcus theory led to a theoretical hole mobility ranging from 6-15 $cm^2V^{-1}s^{-1}$,[12] while recent experimental single crystal FET mobilities [1] reached 15-40 $cm^2V^{-1}s^{-1}$, calling for better theoretical descriptions, since in principle, theoretical value should be considered as an upper

[a] MOE Key Laboratory of Organic Optoelectronics and Molecular Engineering, Department of Chemistry, Tsinghua University, Beijing 100084 (China)
[b] National Center for Nanoscience and Technology, Beijing 100190 (China)
[c] Hubei Collaborative Innovation Center for Advanced Organic, Chemical Materials, and College of Chemistry and Chemical Engineering, Hubei University, Wuhan 430062 (China)
[d] Institute of Chemistry, Chinese Academy of Sciences, Beijing 100190 (China)
[e] Collaborative Innovation Center of Chemistry for Energy Materials, College of Chemistry and Chemical Engineering, Xiamen University, Xiamen 361005 (China)
E-mail: zgshuai@tsinghua.edu.cn; yizhao@xmu.edu.cn.

†This work is supported by National Natural Science Foundation of China (Grant Nos. 21290191, 21303213, 91333202) and the Ministry of Science and Technology of China through 973 program (Grant Nos. 2011CB932304, 2011CB808405, and 2013CB933503).
Electronic Supplementary Information (ESI) available: TDWPD and deformation potential theory calculation details. See DOI: 10.1039/x0xx00000x

limit. The increasing FET mobility trend is due to the improvements in material processes and device fabrications. It is generally believed that the active transport parts of an OFET are just a few molecular layers adjacent to the dielectrics. Due to the gate electric field, impurities or defects within these layers could be easily swept out, making FET mobility in general higher than the bulk materials where the mobility is usually dominated by disorders, impurities or defects, as described by phenomenological model proposed by Bässler.[13]

Our previous efforts of incorporation of the quantum nuclear effect absent in the semiclassical Marcus theory has led to several novel findings, namely: (i) the enhancement of a few fold in mobility values due to the effective lowing of barrier through quantum fluctuation;[11] (ii) mobility decrease with temperature even for localized charge, which provided a more natural explaination for the paradoxical observations by Sakanoue and Sirringhaus that the optical signature of carrier in TIPS-pentacene showed localized charge, but the mobility decreased with temperature, behaving delocalized "bandlike";[14] (iii) negative isotope effect instead of null in semiclassical Marcus theory,[15] which had been unclear at all for decades.[16] Most interestingly, such a localized charge nuclear tunnelling model was adopted to clarify the long-standing disputes over the mechanism of electrical conduction in doped conjugated polymers: nuclear tunnelling assisted hopping was claimed to be a universal description for all the polymers by Asadi *et al.*.[17]

However, either Marcus theory or quantum nuclear tunnelling model which has assumed strong electron localization and weak electron coherence, might not be applicable to recently discovered high mobility materials with indication of bandlike behavior. And in most cases, the transport mechanism is situated in between the localized and the delocalized ends. Mixed quantum/classical dynamics (MQCD) and full quantum dynamics (FQD) methods have been proposed to investigate charge transport. MQCD methods are more efficient but treating nuclear motions by classical dynamics, as represented by the dynamic disorder-limited transport theory [18] based on Su-Schrieffer-Heeger type model parameterized with the aids of first-principles calculation. In contrast, FQD methods can consider nuclear quantum effect, such as nonperturbative hierarchically coupled equations of motion[19] and the non-Markovian stochastic Schrödinger equation.[20] However, most of them are limited to systems with only tens of sites due to the numerical convergence problem and computer memory limitation. Thus, FQD methods are rarely applied to study real OSCs. Zhao *et al.* has recently proposed a more efficient FQD method based on stochastic Schrödinger equation, namely the time-dependent wavepacket diffusion (TDWPD) approach, to study the charge transport property. TDWPD method can deal with hundreds or even thousands orbitals/sites efficiently and the nuclear quantum effect is considered through harmonic oscillator model. For the sake of benchmark, it shows good agreement[21] with path integral method and nonperturbative hierarchically coupled equations of motion[19] for small-sized symmetric systems where the latter can be applied. TDWPD has been proven to be both effective and efficient despite of the difficulty in reproducing Boltzmann distribution for asymmetric systems.[22] This method is introduced in the Method part in this paper.

As far as the complete delocalized bandlike transport is concerned, we have shown previously that the deformation potential theory coupled with the Boltzmann equation can provide a reasonally quantitative description. [23] It was found that the intrinsic bandlike mobility is dominated by scattering with the longitudinal acoustic phonons while the optical phonons and the transverse acoustic phonon processes can be ignored at room temperature.[24]

Carrier (electron or hole) transport in real materials should fall in the range of the above four regimes. In order to better predict the carrier mobility, we present a systematic study on the five typical high mobility OSCs employing all the four models and compare with the available experimental results. These are pentacene, rubrene, dinaphtho-thieno-thiophene (DNTT), Dianthra-thieno-thiophene (DATT), and PDIF-CN2, of which the first four are typical p-type and the latter one is typical n-type materials (Figure 1). All possess layered structure. For simplicity, we investigate only the two-dimensional (2D) transport property and extend to 3D through spatial average.

The crystallographic parameters of the corresponding crystals are listed in Table 1. The charge reorganization energies and the intermolecular electronic couplings for the five crystals are presented in Table 2. The directions of the corresponding charge transitions are drawn in Figure 2. For all the systems, the significant charge transitions are coplanar in one certain plane, which is *bc* plane for rubrene and *ab* plane for the rest, demonstrating 2D carrier transport property. Therefore, we use different models to calculate the carrier mobility respectively.

We first investigate the angular dependences of the mobility by Marcus hopping model, quantum nuclear tunnelling model, as well as TDWPD method, which have been plotted in Figure 3. The theoretical results show that the three random walk simulation based methods present very similar anisotropic behaviors. Among the five organic crystals, rubrene

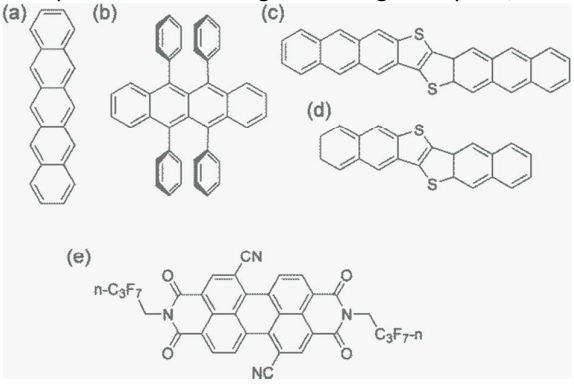

Figure 1. The molecular structures of high-mobility OSCs studied in this work: (a) pentacene, (b) rubrene, (c) DNTT, (d) DATT, (e) PDIF-CN2.

Table 1. Lattice constants and angles for the unit cells of all calculated crystals.

	a (Å)	b (Å)	c (Å)	α (°)	β (°)	γ (°)	Ref.
Pentacene	6.27	7.78	14.53	76.48	87.68	84.68	[25]
Rubrene	26.86	7.19	14.43	90.00	90.00	90.00	[26]
DATT	6.26	7.57	20.83	90.00	92.78	90.00	[3b]
DNTT	6.19	7.66	16.21	90.00	92.49	90.00	[27]
PDIF-CN2	5.23	7.64	18.82	92.51	95.25	104.73	[28]

Table 2. The electronic couplings (V) with non-zero value and the total reorganization energy (λ) in the five crystals.

meV	Pentacene	rubrene	DATT	DNTT	PDIF-CN2
***V*1**	32.6	83.0	66.8	67.2	95.2
***V*2**	47.0	14.1	38.4	86.1	0.1
***V*3**	77.1	1.2	84.8	20.5	65.0
***V*4**	29.9	0.1	2.2	2.5	
***V*5**	3.4		0.2	0.3	
λ	91	151	86	131	277

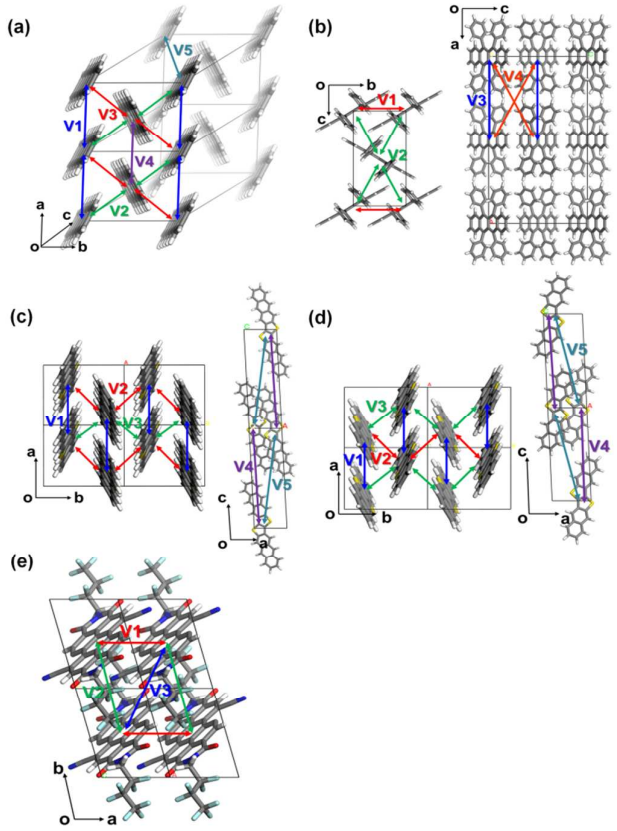

Figure 2. The most important hopping paths in the five crystals: (a) pentacene, (b) rubrene, (c) DNTT, (d) DATT, (e) PDIF-CN2.

possesses the strongest anisotropic transport property ($\mu_b \sim 15\mu_a$), which is due to the much larger electronic coupling along b direction ($V1$) than others. On the other hand, pentacene, DATT and DNTT own the weakest anisotropic property where $\mu_a < 2\mu_b$. The strong anisotropy in rubrene and weak anisotropy in DNTT match well with experiments,[3c, 29] indicating the reliability of random walk simulation.

For better understanding the transport mechanism, we then calculate the average mobilities by the four methods mentioned previously as listed in Table 3. For comparing with experiment, the averaged 3D mobilities are also presented. The bandlike mobility calculated with DP theory coupled with Boltzmann transport equation represent the full delicalization, which usually give much larger mobility value. The results of pentacene,[6c] DATT[6b] and DNTT[6b] are quoted from references, while others are calculated according to the methodology presented in reference,[23] and the calculation details are shown in the supporting information. It should be noted that only acoustic phonon scattering is included in DP theory and optical phonon is excluded. Xi *et al.*[24] used Wannier-interpolation method to calculate the band mobility in 2D carbon materials considering both acoustic and optical phonons, and they found that the main scattering mechanism is acoustic phonons, while the optical phonons only play some roles at high temperatures or at low electron energies. Therefore, it is feasible to apply DP theory on studying the band transport behavior. The mobilities resulted from the four methods show that the DP mobility (μ_{DP}) is the largest for all the systems. Especially for rubrene, DATT, DNTT and PDIF-CN2, their DP mobilities are one order of magnitude larger than other theoretical mobilities as well as experimental results. Therefore, the rationality of describing the charge transport in organic systems by bandlike model should be questioned, and further theoretical and experimental studies are needed. As we have explained before,[14] the so-called bandlike decreasing temperature behavior could arise from the nuclear tunnelling effect for a localized state, instead of delocalization effect.

The sequence of mobility values resulted from other three methods for each system is: $\mu_{TDWPD} > \mu_{Quantum} > \mu_{Marcus}$. It is natural that both nuclear quantum effect and electron coherence can facilitate carrier transport. With comparing experimental results, Marcus theory underestimates the mobility for all the systems, even though the molecular parameters themselves are useful for molecular design stressed by Brédas *et al.* who did not try to make quantitative prediction of mobility through Marcus theory, but evaluated the molecular parameters which were pertinent to material design.[10] To the contrary, both quantum model and TDWPD method with nuclear tunnelling effect seem to be able to give reasonable results compared to experiments, illustrating the significance of nuclear tunnelling effect on charge transport.

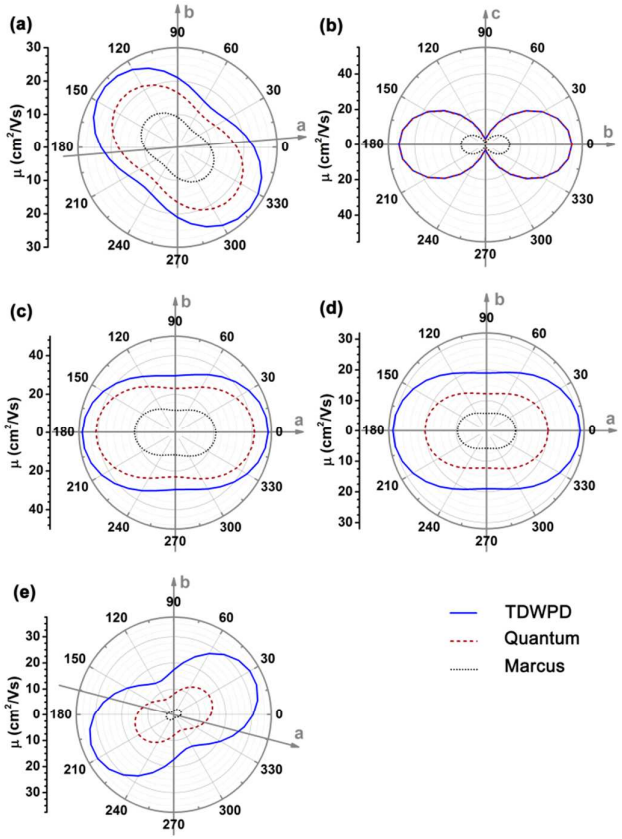

Figure 3. The anisotropic carrier mobilities obtained from TDWPD method, quantum nuclear tunnelling model, and Marcus model in the five crystals: (a) pentacene, (b) rubrene, (c) DNTT, (d) DATT, (e) PDIF-CN2.

Table 3. The theoretical mobility (μ) along axes (*a*, *b*, or *c* direction) and the 3D averaged (AVG) mobility obtained from Marcus model, quantum nuclear tunnelling model, TDWPD method, as well as deformation potential (DP) theory. The experimental results are also given for comparison.

μ ($cm^2V^{-1}s^{-1}$)	Marcus	Quantum	TDWPD	DP	Exp.
Pentacene	*a*: 9.4	*a*: 16.9	*a*: 21.8	*a*: 58.0	15~40 [1]
	b: 9.3	*b*: 16.7	*b*: 21.1	*b*: 44.0[6c]	
	AVG: 6.7	AVG: 11.8	AVG:15.1		
Rubrene	*b*: 13.8	*b*: 48.9	*b*: 49.0	*b*: 242.6	15~17 [2a]
	c: 0.8	*c*: 2.8	*c*: 3.2	*c*: 72.7	
	AVG: 4.9	AVG: 17.2	AVG: 17.4		
DATT	*a*: 21.2	*a*: 41.3	*a*: 48.3	*a*: 322.6	16[10c]
	b: 11.6	b: 23.0	*b*: 29.6	*b*: 19.1[6b]	
	AVG: 10.6	AVG: 21.1	AVG: 25.2		
DNTT	*a*: 9.5	*a*: 20.2	*a*: 30.7	*a*: 137.7	6.8~7.5[3c]
	b: 5.8	*b*: 12.2	*b*: 19.0	*b*: 76.4[6b]	
	AVG: 5.1	AVG: 10.7	AVG: 16.3		
PDIF-CN2	*a*: 2.3	*a*: 12.1	*a*: 25.9	*a*: 132.8	1~6[30]
	b: 1.5	*b*: 8.0	*b*: 17.4	*b*: 91.2	
	AVG: 1.4	AVG: 7.5	AVG: 16.1		

The step beyond the Marcus theory is an extension to consider the nuclear quantum effect. Here, we simply regard the ratio of quantum mobility and Marcus mobility ($\mu_{Quantum}/\mu_{Marcus}$) as representing the nuclear quantum effect, and we find that the nuclear quantum effect is directly determined by charge reorganization energy, seen in Figure 4. As the reorganization energy increases, the scattering of intramolecular nuclear vibrations on electron is strengthened, leading to smaller mobility. However, the nuclear quantum effect can linearly increase with reorganization energy. The results show that the nuclear tunnelling can at least double Marcus mobility, so that nuclear tunnelling effect cannot be neglected during charge transport process for organic semiconductors.

As mentioned before that Eq. (1) can be derived from Eq. (2) with two approximations, namely the short-time approximation (STA) and the high temperature assumption (HTA). These two lead to the classical limit. We now consider the mobility values using quantum CT rate with only STA, to investigate the inhibitions of STA and HTA on nuclear tunnelling effect, which reads

$$k^{STA} = \frac{V^2}{\hbar^2}\sqrt{\frac{2\pi}{\sum_j S_j\omega_j^2\left(2\bar{n}_j+1\right)}}\exp\left[-\frac{\left(\sum_j S_j\omega_j\right)^2}{2\sum_j S_j\omega_j^2\left(2\bar{n}_j+1\right)}\right] \quad (3)$$

The STA and HTA effects can be represented by $\mu_{Quantum}/\mu_{STA}$ and μ_{STA}/μ_{Marcus} separately, and their values of all systems are also shown in the inset of Figure 4. As λ increases, the STA effect slightly decreases while HTA effect increases. Thus, it is HTA that make the major contribution to the diminishing of nuclear tunnelling effect when λ > ca. 160 meV. Therefore, we caution the application of the semiclassical Marcus theory for organic semiconductor for quantitative assessment of mobility since the approximations are not justified.

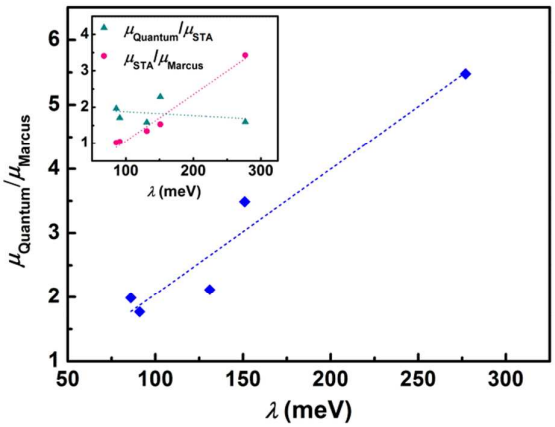

Figure 4. The relationship between reorganization energy (λ) and $\mu_{Quantum}/\mu_{Marcus}$ for all the systems. The relationships between λ and $\mu_{Quantum}/\mu_{STA}$ as well as μ_{STA}/μ_{Marcus} are also presented in the inset.

TDWPD method can consider both the electronic coherence with delocalization effects and the quantum nature of nuclear motion through harmonic oscillator model. It is seen from Table 3, the mobility obtained by TDWPD is always larger than that from quantum nuclear tunnelling model. The electronic coherence length can be measured by non-diagonal component $<c_i c_j>$.[31] For the sake of simplicity, here we only consider the real part of the fluctuation in the correlation function. In fact, it is found that the particle dynamics caused by the ignorance of imaginary fluctuation has been proved to be small.[21] Charge population propagation on the initial site can qualitatively measure the coherence motion of charge carrier which is given in Figure S1. It is found that the charge populations of all systems start to decay with oscillation behavior within a period of 1000 a.u. (24 fs), which describes the coherent motion of charge. However, beyond that point, the quasi-thermal-equilibrium of diffusions can be obtained (Figure S2), and the population oscillating behavior disappears, indicating that the electronic coherence is loosing. Therefore, we attribute the larger mobility achieved by TDWPD than nuclear tunnelling model to the electronic delocalization effect rather than electronic coherence.

The electronic delocalization for the five systems at 24 fs is illustrated in Figure 5. It is found that rubrene possesses the shortest delocalization length among all systems, even though its reorganization energy and transfer integral are similar to those in DNTT. The delocalization length of the latter is more than twice longer than that of rubrene. This is due to the strong anisotropy for *V* in rubrene crystal, as seen from Table 2. The 1D-like behavior leads to relatively small charge delocalization. Thus, the mobility values from quantum hopping model and the TDWPD method are very close to each other. However, for the other four systems, the charge delocalization effect is seen to be significant. It is also noted that the computed mobility values from a complete delocalized bandlike model as simulated with DP theory are well overestimated compared with experiments, demonstrating the inappropriateness of bandlike picture for OSCs.

To summarize, we adopt four methods from hopping to bandlike mechanisms to investigate the intrinsic charge transport property of several organic semiconductors with high mobility. In general, the semiclassical Marcus theory underestimates the mobility due to the ignorance of nuclear quantum effect, while the bandlike deformation potential theory always overestimates the mobility because of the neglect of the charge localization effect, especially for rubrene, DATT, DNTT and PDIF-CN2. Both quantum nuclear tunnelling model and TDWPD method can give appropriate descriptions for these high mobility organic materials, implying polaron transport assisted by nuclear tunnelling is universal for organic materials including conducting polymers. Compared $\mu_{Quantum}$ with μ_{Marcus}, we find that the larger reorganization energy will lead to stronger nuclear tunnelling effect, so that $\mu_{Quantum}/\mu_{Marcus}$ becomes larger. TDWPD method contains both electronic coherence and delocalization effects in addition to quantum nuclear effect. TDWPD calculations demonstrate that

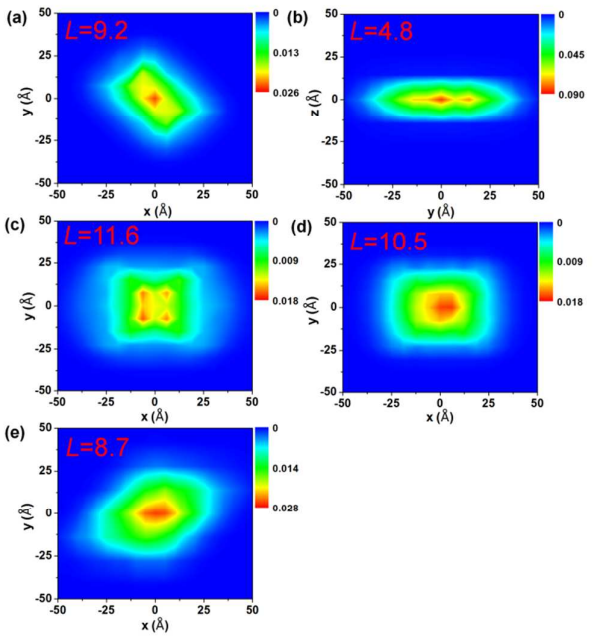

Figure 5. The charge population distributions of all systems at 24 fs: (a) pentacene, (b) rubrene, (c) DNTT, (d) DATT, (e) PDIF-CN2. The 2D electronic delocalization length (*L*) labelled in each picture is calculated by $L=\sqrt{1/\sum_{i=1}|c_i|^4}$.

the electronic coherence is not significant in the determination of charge transport mobility, while electronic delocalization plays an important role, and delocalization effect can facilitate transport. When electronic delocalization effect is relatively strong, wavepacket description with nuclear tunnelling effect is more appropriate, for example, in pentacene, DATT, DNTT and PDIF-CN2. While for the systems with weak electronic delocalization like rubrene, a simple nuclear tunnelling enabled hopping model is sufficient.

Methods

The method of random walk simulation based on Marcus theory was summarized in ref. [10d]. And the nuclear tunnelling method was presented in Ref. [11] and [14]. And the bandlike DP methodology and computational details are given in supporting information S2. TDWPD method is relatively new, so we give a brief introduction here. After an electron is injected into a molecule in the organic crystal, it hops or coherently moves to another. Its CT process is determined by the intermolecular transfer integral and the thermal vibration of molecules which is taken into account by allowing the site energy ε_{ii} and the transfer integral ε_{ij} to fluctuate in time. The corresponding Hamiltonian can be express as

$$H(t)=\sum_{i=1}^{N}(\varepsilon_{ii}+F_i(t))|i\rangle\langle i|+\sum_{i\neq j}^{N}(\varepsilon_{ij}+V_{ij}(t))|i\rangle\langle j| \quad (4)$$

Here $|i\rangle$ corresponds to the electronic state of the *i*-th site, and $F_i(t)$ and $V_{ij}(t)$ represent the fluctuations of site energy and transfer integral respectively. In this work, we mainly focus on

the nuclear tunnelling effect resulted from intramolecular vibrations. Moreover, since several theoretical researches indicate that their 2D transport property of organic semiconductors is nearly unaffected by lattice dynamic disorder.[22, 32] Thus the fluctuation of transfer integral caused by lattice dynamics is not considered here.

To obtain the memory effect of site energy fluctuation, we need the spectral density function of the electron-phonon interaction which can be written as $J(\omega)=\frac{\pi}{2}\sum_j \frac{\chi_j^2}{\omega_j}\delta(\omega-\omega_j)$. Here the electron-phonon interaction strength of *j*-th normal mode is $\chi_j=\Delta Q_j\omega_j^2$. The δ function is evaluated with Lorentz distribution $\delta(\omega-\omega_j)=\frac{1}{\pi}\frac{a}{a^2+(\omega-\omega_j)^2}$. Once *J*(ω) is known, the site energy fluctuation can be achieved by $F_i(t)=\sum_{n=1}^{N}\left[2G(\omega_n)\Delta\omega\right]^{1/2}\cos(\omega_n t+\phi_n)$. Here, $G(\omega)=J(\omega)\coth(\beta^T\omega/2)/\pi$ is the modified spectral density function at a special temperature *T* ($\beta=1/k_BT$) to make it satisfy the detailed balance principle. $\Delta\omega=\omega_{\max}/N$, where $\omega_{\max}$ is the upper cutoff frequency, and $\omega_n=n\Delta\omega$. ϕ_n is the independent random phase which is uniformly distributed over the interval [0, 2π].

To describe the electronic dynamics, the time-dependent Schrödinger equation is solved with Chebyshev polynomial expansion technique.[33] Once the wave function of system $\psi(t)=\sum_i^N c_i(t)|i\rangle$ is known, the time-dependent electronic properties can be easily obtained. The diffusion coefficient *D* can be achieved by $D=\lim_{t\to\infty}\frac{\langle R^2(t)\rangle}{2dt}$ where $\langle R^2(t)\rangle=\sum_i^N r_i^2\rho_{ii}(t)$ will grow linearly with time *t* after some time, and *d* represents the number of dimensions. The origin is defined as $\langle R^2(0)\rangle=0$, and one charge is completely localized on one site *a*. r_i is the distance from site *i* to site *a*, and $\rho_{ii}(t)=\langle c_i^*(t)c_i(t)\rangle$ is the charge population on site *i*, which averages over 400 independent trajectories here.

In Eqs. (1), (2) or (4), the intermolecular transfer integral *V* between molecules *m* and *n* is calculated with the site-energy corrected coupling method[34] which can be expressed as $V_{mn}=\frac{V_{mn}^0-\frac{1}{2}(e_m+e_n)O_{mn}}{1-O_{mn}^2}$, where $e_m=\langle\phi_m|H|\phi_m\rangle$, $V_{mn}^0=\langle\phi_m|H|\phi_n\rangle$ and $O_{mn}=\langle\phi_m|O|\phi_n\rangle$. $\phi_{m(n)}$ is the frontier molecular orbital of an isolated molecule *m (n)* in the dimer. For hole (electron) transport, the HOMO (LUMO) should be plugged in. *H* and *O* are the dimer Hamiltonian and the overlap matrices respectively.

For Marcus and nuclear tunnelling models, the charge mobility can be obtained by assuming a diffusion process by virtue of Einstein formula $\mu=eD/k_BT$ after achieving the CT rate from one molecule to each neighbour. The diffusion constant *D* is simulated by a random walk by kinetic Monte Carlo simulation. The charge hops between nearest-neighbouring molecules with a probability $p_\alpha=k_{mn}^\alpha/\sum_\alpha k_{mn}^\alpha$ for the *α*-th pathway, and the simulation time is incremented by $1/\sum_\alpha k_{mn}^\alpha$.[35] The diffusion coefficient can also be obtained by $D=\lim_{t\to\infty}\frac{\langle R^2(t)\rangle}{2dt}$ averaging over 8000 trajectories. We repeat 100 times, and the average mobility is evaluated as $\frac{1}{100}\sum_i^{100}\mu_i$.

The reorganization energy and the electronic coupling necessary for Marcus theory, quantum nuclear tunnelling model and TDWPD method are determined by quantum chemical first-principles calculations. Density functional theory (DFT) is adopted as implemented in Gaussian 09 package.[36] The neutral and charged geometries of all systems are optimized with B3LYP functional[37] and 6-31G(d) basis set, and vibrational frequencies are calculated at the same level. With the help of DUSHIN program,[38] the corresponding Huang-Rhys factor and reorganization energy of each vibrational mode entered in Eq. (2) are obtained under the displaced harmonic oscillator approximation. Then, the spectral density function needed in TDWPD method can be derived. For the intermolecular transfer integral *V* for all the neighboring molecular pairs, the PW91PW91 functional[39] plus a 6-31G(d) basis set is employed. All mobility calculations are carried out at 300 K. The clusters used for TDWPD calculations for all systems are 41×41 2D clusters.

Notes and references

1 O. D. Jurchescu, M. Popinciuc, B. J. van Wees, and T. T. M. Palstra, *Adv. Mater.* **2007**, *19*, 688.
2 a) W. Xie, K. A. McGarry, F. Liu, Y. Wu, P. P. Ruden, C. J. Douglas, and C. D. Frisbie, *J. Phys. Chem. C* **2013**, *117*, 11522; b) R. Zeis, C. Besnard, T. Siegrist, C. Schlockermann, X. Chi, and C. Kloc, *Chem. Mater.* **2005**, *18*, 244; c) V. Podzorov, E. Menard, A. Borissov, V. Kiryukhin, J. A. Rogers, and M. E. Gershenson, *Phys. Rev. Lett.* **2004**, *93*, 086602.
3 a) H. Ebata, T. Izawa, E. Miyazaki, K. Takimiya, M. Ikeda, H. Kuwabara, and T. Yui, *J. Am. Chem. Soc.* **2007**, *129*, 15732; b) K. Niimi, S. Shinamura, I. Osaka, E. Miyazaki, and K. Takimiya, *J. Am. Chem. Soc.* **2011**, *133*, 8732; c) W. Xie, K. Willa, Y. Wu, R. Häusermann, K. Takimiya, B. Batlogg, and C. D. Frisbie, *Adv. Mater.* **2013**, *25*, 3478; d) M. J. Kang, I. Doi, H. Mori, E. Miyazaki, K. Takimiya, M. Ikeda, and H. Kuwabara, *Adv. Mater.* **2011**, *23*, 1222; e) K. Takimiya, S. Shinamura, I. Osaka, and E. Miyazaki, *Adv. Mater.* **2011**, *23*, 4347.
4 T. He, M. Stolte, and F. Würthner, *Adv. Mater.* **2013**, *25*, 6951.

5 N. A. Minder, S. Ono, Z. Chen, A. Facchetti, and A. F. Morpurgo, *Adv. Mater.* **2012**, *24*, 503.
6 a) L. Tang, M. Long, D. Wang, and Z. Shuai, *Sci. China Series B: Chemistry* **2009**, *52*, 1646; b) J. Xi, M. Long, L. Tang, D. Wang, and Z. Shuai, *Nanoscale* **2012**, *4*, 4348; c) H. Kobayashi, N. Kobayashi, S. Hosoi, N. Koshitani, D. Murakami, R. Shirasawa, Y. Kudo, D. Hobara, Y. Tokita, and M. Itabashi, *J. Chem. Phys.* **2013**, *139*, 014707.
7 O. Ostroverkhova, D. G. Cooke, S. Shcherbyna, R. F. Egerton, F. A. Hegmann, and R. R. Tykwinski, J. E. Anthony, *Phys. Rev. B* **2005**, *71*, 035204.
8 V. Podzorov, E. Menard, J. A. Rogers, and M. E. Gershenson, *Phys. Rev. Lett.* **2005**, *95*, 226601.
9 T. Sakanoue, and H. Sirringhaus, *Nat. Mater.* **2010**, *9*, 736.
10 a) J. L. Brédas, J. P. Calbert, D. A. da Silva Filho, and J. Cornil, *Proc. Natl. Acad. Sci. USA* **2002**, *99*, 5804; b) J. Cornil, D. Beljonne, J. P. Calbert, and J. L. Brédas, *Adv. Mater.* **2001**, *13*, 1053; c) V. Coropceanu, J. Cornil, D. A. da Silva Filho, Y. Olivier, R. Silbey, and J.-L. Brédas, *Chem. Rev.* **2007**, *107*, 926; c) A. N. Sokolov, S. Atahan-Evrenk, R. Mondal, H. B. Akkerman, R. S. Sánchez-Carrera, S. Granados-Focil, J. Schrier, S. C. Mannsfeld, A. P. Zoombelt, and Z. Bao, *Nat. commun.* **2011**, *2*, 437; d) L. J. Wang, G. Nan, X. D. Yang, Q. Peng, Q. Li, and Z. Shuai, Chem. Soc. Rev. **2010**, *39*, 423.
11 G. Nan, X. Yang, L. Wang, Z. Shuai, and Y. Zhao, *Phys. Rev. B* **2009**, *79*, 115203.
12 W. Q. Deng, and W. A. Goddard III, *J. Phys. Chem. B* **2004**, *108*, 8614.
13 H. Bässler , *Phys. Status Solidi B* **1993** , *175* , 15.
14 H. Geng, Q. Peng, L. Wang, H. Li, Y. Liao, Z. Ma, and Z. Shuai, *Adv. Mater.* **2012**, *24*, 3568.
15 a) Y. Jiang, H. Geng, W. Shi, Q. Peng, X. Zheng, and, Z. Shuai, *J. Phys. Chem. Lett.* **2014**, *5*, 2267; b) Y. Jiang, Q. Peng, H. Geng, H. Ma, and Z. Shuai, *Phys. Chem. Chem. Phys.* **2015**, *17*, 3273.
16 a) R. W. Munn, J. R. Nicholson, W. Siebrand, and D. F. Williams, *J. Chem. Phys.* **1970**, *52*, 6442; b) R. W. Munn, and W. Siebrand, *J. Chem. Phys.* **1970**, *52*, 6391.
17 K. Asadi, A. J. Kronemeijer, T. Cramer, L. Jan Anton Koster, P. W. M. Blom, and D. M. de Leeuw, *Nat. Commun.* **2013**, *4*, 1710.
18 A. Troisi, and G. Orlandi, *Phys. Rev. Lett.* **2006**, *96*, 086601.
19 D. Wang, L. Chen, R. Zheng, L. Wang, and Q. Shi, *J. Chem. Phys.* **2010**, *132*, 081101.
20 X. Zhong, Y. Zhao, *J. Chem. Phys.* **2013**, *138*, 014111.
21 X. Zhong, and Y. Zhao, *J. Chem. Phys.* **2011**, *135*, 134110.
22 W. Zhang, X. Zhong, and Y. Zhao, *J. Phys. Chem. A* **2012**, *116*, 11075.
23 W. Shi, J. Chen, J. Xi, D. Wang, and Z. Shuai, *Chem. Mater.* **2014**, *26*, 2669-2677.
24 J. Xi, D. Wang, Y. Yi, and Z. Shuai, *J. Chem. Phys.* **2014**, *141*, 034704.
25 C. C. Mattheus, A. B. Dros, J. Baas, A. Meetsma, J. L. de Boer, and T. T. M. Palstra, *Acta Crystallogr. Sect. C: Cryst. Struct. Commun.* **2001**, *57*, 939.
26 O. D. Jurchescu, A. Meetsma, and T. T. Palstra, *Acta Crystallogr. Sect. B: Struct. Sci.* **2006**, *62*, 330.
27 T. Yamamoto, and K. Takimiya, *J. Am. Chem. Soc.* **2007**, *129*, 2224.
28 B. A. Jones, M. J. Ahrens, M.-H. Yoon, A. Facchetti, T. J. Marks, and M. R. Wasielewski, *Angew. Chem. Inter. Ed.* **2004**, *43*, 6363.
29 a) V. C. Sundar, J. Zaumseil, V. Podzorov, E. Menard, R. L. Willett, T. Someya, M. E. Gershenson, and J. A. Rogers, *Science* **2004**, *303*, 1644-1646; b) M.-M. Ling, C. Reese, A. L. Briseno, and Z. Bao, *Synth. Met.* **2007**, *157*, 257.
30 A. S. Molinari, H. Alves, Z. Chen, A. Facchetti, and A. F. Morpurgo, *J. Am. Chem. Soc.* **2009**, *131*, 2462.
31 Y. Zhao, *J. Theor. Comp. Chem.* **2008**, *7*, 869.
32 a) L. Wang, Q. Li, Z. Shuai, L. Chen, and Q. Shi, *Phys. Chem. Chem. Phys.* **2010**, *12*, 3309-3314; b) G. Nan, and Z. Li, *Phys. Chem. Chem. Phys.* **2012**, *14*, 9451.
33 a) H. Talezer, and R. Kosloff, *J. Chem. Phys.* **1984**, *81*, 3967; b) C. Leforestier, R. H. Bisseling, C. Cerjan, M. D. Feit, R. Friesner, A. Guldberg, A. Hammerich, G. Jolicard, W. Karrlein, H. D. Meyer, N. Lipkin, O. Roncero, and R. Kosloff, *J. Comp. Phys.* **1991**, *94*, 59-80.
34 E. F. Valeev, V. Coropceanu, D. A. da Silva Filho, S. Salman, and J.-L. Brédas, *J. Am. Chem. Soc.* **2006**, *128*, 9882.
35 W. M. Young, and E. W. Elcock, *Proc. Phys. Soc.* **1966**, *89*, 735.
36 M. J. Frisch, et al, Revision D.01 ed., Gaussian Inc., Wallingford CT, **2009**.
37 a) A. D. Becke, *J. Chem. Phys.* **1993**, *98*, 5648; b) C. Lee, W. Yang, and R. G. Parr, *Phys. Rev. B* **1988**, *37*, 785.
38 J. R. Reimers, *J. Chem. Phys.* **2001**, *115*, 9103.
39 J. P. Perdew, J. A. Chevary, S. H. Vosko, K. A. Jackson, M. R. Pederson, D. J. Singh, and C. Fiolhais, *Phys. Rev. B* **1992**, *46*, 6671.